A dual-application poly (DL-lactic-co-glycolic) acid (PLGA)-chitosan composite scaffold for potential use in bone tissue engineering

Yamina Boukari[a] (yamina.boukari@gmail.com), Omar Qutachi[b] (omar.qutachi@nottingham.ac.uk), David J. Scurr[b] (david.scurr@nottingham.ac.uk), Andrew P. Morris[a] (andrew.morris@nottingham.edu.my), Stephen W. Doughty[c] (stephen.doughty@pmc.edu.my), and Nashiru Billa[a*]

[a]School of Pharmacy, The University of Nottingham Malaysia Campus, Jalan Broga, 43500 Semenyih, Selangor, Malaysia.

[b]School of Pharmacy, The University of Nottingham, Park Campus, Nottingham NG7 2RD, United Kingdom.

[c]Penang Medical College, 4 Jalan Sepoy Lines, 10450 George Town, Penang, Malaysia

*Corresponding author: Nashiru.Billa@nottingham.edu.my; Tel, +60389248211; Fax, +60389248018

Abstract

The development of patient-friendly alternatives to bone-graft procedures is the driving force for new frontiers in bone tissue engineering. Poly ($_{\mathrm{DL}}$-lactic-co-glycolic acid), (PLGA) and chitosan are well-studied and easy-to-process polymers from which scaffolds can be fabricated. In this study, a novel dual-application scaffold system was formulated from porous PLGA and protein-loaded PLGA/chitosan microspheres. Physicochemical and *in vitro* protein release attributes were established. The therapeutic relevance, cytocompatibility with primary human mesenchymal stem cells (hMSCs) and osteogenic properties were tested. There was a significant reduction in burst release from the composite PLGA/chitosan microspheres compared with PLGA alone. Scaffolds sintered from porous microspheres at 37°C were significantly stronger than the PLGA control, with compressive strengths of 0.846 ± 0.272 MPa and 0.406 ± 0.265 MPa, respectively ($p < 0.05$). The formulation also sintered at 37°C following injection through a needle, demonstrating its injectable potential. The scaffolds demonstrated cytocompatibility, with increased cell numbers observed over an 8-day study period. Von Kossa and immunostaining of the hMSC-scaffolds confirmed their osteogenic potential with the ability to sinter at 37°C *in situ.*

Keywords: polymeric biomaterials, controlled delivery, poly (lactic-co-glycolic acid) (PLGA), microspheres, protein delivery, tissue engineering, mechanical properties, formulation.[1]

---

[1]Abbreviations

BMPs, bone morphogenetic proteins; BSA, bovine serum albumin; DCM, dichloromethane; DMSO, dimethyl sulphoxide; ECM, extracellular matrix; FTIR, Fourier transform infrared; hMSC, primary human mesenchymal stem cells; PBS, phosphate-buffered saline; PLGA, poly (lactic-co-glycolic acid); PVA, poly (vinyl alcohol); SDS, sodium dodecyl sulphate; SEM, scanning electron microscopy, TPP, sodium tripolyphosphate; ToF-SIMS, time of flight secondary ion mass spectroscopy.

1. Introduction

There is an urgent need for alternative approaches for the regeneration of bone following fracture or orthopaedic damage *in lieu* of traditional methods, and these alternative approaches constitute an important tissue engineering application (Vo et al., 2012). The current ‘gold standard’ therapy is the bone graft procedure, which involves taking autologous bone, usually harvested from the iliac crest of the patient, and implanting it into their defect site (Martino et al., 2012; Amini et al., 2013). Alternatively, allograft bone from donors or cadavers can be extracted from the femoral heads or extremities of other long bones (Delloye et al., 2007). This implanted tissue acts as a scaffold for the existing bone tissue to infiltrate and deposit extracellular matrix (ECM), leading to the remodelling of the fractured bone (Bostrom and Mikos, 1997). Numerous drawbacks are associated with the above procedures, including the limited supply of autologous bone, complications at the donor site and high surgical costs (Martino et al., 2012). Furthermore, in large defects, resorption may occur before osteogenesis has been completed (Burg et al.,2000). Allograft bone usage is associated with incompatibility with the host, and the possible transmission of diseases and infections such as hepatitis and HIV (Vo et al., 2012; Bostrom and Mikos, 1997; Chen et al., 2010; Puppi 2010). The risk of disease transmission from allograft bone can be minimised by processing or devitalization via freeze-drying or irradiation; however, this may reduce the osteoinductivity and mechanical strength (White et al., 2013; Hau et al., 2008; Nauth et al., 2011). Other options include the usage of bone morphogenetic proteins (BMPs), distraction osteogenesis and bone cement; however, these are also not ideal (Amini et al., 2013). The shortcomings in the current clinical options have led to concerted efforts in search of alternative strategies for the repair of bone.

Poly ($_{DL}$-lactic-co-glycolic acid) (PLGA) is a well-studied synthetic polymer used in bone tissue engineering. It has favourable properties such as biodegradability (Pan and Ding, 2012), cytocompatibility, controllable mechanical properties (Bostrom and Mikos, 1997; Burg et al., 2000; Chen et al., 2010; Puppi et al., 2010) and it can be easily processed (Burg et al., 2000; Pan and Ding, 2012). Furthermore, PLGA has been approved by the FDA for use in certain clinical applications (Lu et al., 2009).

The combination of porous and non-porous microspheres, which are able to sinter at body temperature, enables the introduction of porosity within injected scaffolds, hence, allowing proliferating cells access to nutrients [Qutachi et al., 2014; Boukari et al., 2015). Simultaneously, the delivery of growth factors such as BMPs to the growing cells is also facilitated. BMPs have been studied for their use in non-union bone defects, spinal fusion and open tibial fractures (Boukari et al., 2015; Whilte et al., 2013; Hau and Wang, 2008). Furthermore, it has been reported that one such BMP, BMP-2, is present during the initial phase of fracture repair, and during chondrogenesis and osteogenesis (Patel et al., 2008).

Various strategies have been utilized for the sintering of microspheres into scaffolds. These include the incorporation of plasticizers in order to reduce polymer glass transition temperatures (Dhillon et al., 2011), the addition of organic solvents such as dichloromethane (Pan and Ding, 2012; Wang et al., 2010) and the application of heat (Delloye et al., 2007; Chen et al., 2010; Puppi et al, 2010). Although the use of high temperatures and organic solvents result in mechanically strong scaffolds, these conditions are not ideal for the body and so are not suitable for sintering *in-situ*. Therefore, a system capable of sintering at 37°C *in situ* would be extremely beneficial.

Protein-loaded PLGA microspheres often exhibit an initial burst release (Boukari et al., 2015; Tao et al., 2014) which is not ideal for an intended controlled release of BMP-2 at a defect site. A number of strategies have been employed to control the release of proteins from PLGA microspheres. These include varying the polymer molecular weight (Boukari et al., 2015), the inclusion of additives such as poloxamer 188 (Paillard-Giteau et al., 2010) and the use of a PLGA-PEG-PLGA triblock polymer (White et al., 2013; Kirby et al., 2011).

Chitosan is a natural polysaccharide derived from chitin and is popular in tissue engineering applications for a variety of reasons, which include its cytocompatibility and ability to promote cell adhesion (Amini et al., 2012). Chitosan microspheres show promise for use in the encapsulation of proteins and have previously been shown to retain the activity of a neural growth factor (Zeng et al., 2011). Moreover, due to its cationic nature and propensity to slow degradation, chitosan-based materials are able to sustain the release of growth factors (Qian and Zhang, 2013). Chitosan has been used in combination with PLGA in various forms, including by embedding PLGA microspheres into chitosan scaffolds (Kirby et al., 2011; Zeng et al., 2011; Di Martino et al., 2005; Qian, 2013). PLGA/chitosan microspheres can be formulated in a variety of ways. These include the use of supercritical fluid technology (Cassetari et al., 2011), the double emulsion method (Fu et al., 2012; Hu et al., 2008) the solvent evaporation technique (Jian et al., 2010), an electro-dropping layer-by-layer approach (Choi et al., 2013) and conjugation and adsorption methods (Chakravarthi and Robinson, 2011). Porous microspheres have also been treated with chitosan (Yue et al., 2015) (Chakravarthi and Robinson, 2011), whilst others have encapsulated protein-loaded chitosan microspheres into large porous PLGA microspheres (Tao et al., 2014).

In a previous study, we reported the formulation of a novel PLGA scaffold delivery system based on porous and protein-loaded microspheres that sintered at 37°C (Boukari et al., 2015). There have been a number of reports utilising composites of PLGA/chitosan microspheres for use in bone tissue engineering (Casettari et al., 2011; Han et al., 2015; Pandey et al., 2013; Jiang et al., 2010; Choi et al., 2013; Chakravarthi and Robinson, 2011). In the present work, we report the development of a ‘dual-application’ PLGA/chitosan composite scaffold formulation which sinters at 37°C when injected through a hypodermic needle as well as when implanted as a paste. Furthermore, we aimed to control the release kinetics of a model protein for BMP-2 (BMP-2 itself was not used due to the cost implications) from this system, via the inclusion of chitosan, and to investigate its cytocompatibility and osteoinductive capabilities on primary human mesenchymal stem cells (hMSCs).

2. Materials and methods

2.1 Materials

PLGA (85:15, 53 kDa) was purchased from Evonik (Morris, NJ, USA). Chitosan, low molecular weight, ≥ 75% deacetylation; sodium tripolyphosphate (TPP); poly vinyl alcohol (PVA), 87–89% hydrolysed; phosphate buffered saline (PBS; 0.01 M phosphate buffer, 0.0027 M potassium chloride and 0.137 M sodium chloride; pH 7.4) tablets; sodium hydroxide (NaOH) pellets; Triton X-100; goat serum; Hoechst 33258; sodium thiosulphate solution; silver nitrate solution; formalin 10% v/v and paraformaldehyde 10% v/v solutions were purchased from Sigma-Aldrich (St. Louis, MO, USA). Glacial acetic acid was purchased from R&M Chemicals (Essex, UK). Dichloromethane (DCM), dimethyl sulfoxide (DMSO) and sodium dodecyl sulphate (SDS) were purchased from Fisher Scientific UK (Loughborough, UK). Bovine serum albumin (BSA) was purchased from Nacalai Tesque (Kyoto, Japan). A micro BCA protein assay kit was purchased from Thermo Fisher Scientific (Waltham, MA, USA). For stem cell culture, hMSCs, an MSCGM hMSC SingleQuot kit, trypsin/EDTA for MSC and HEPES buffered saline were purchased from Lonza (Basel, Switzerland). Presto Blue cell viability reagent was purchased from Gibco, Life Technologies (Carlsbad, CA, USA). For immunostaining, anti-osteocalcin polyclonal antibody was purchased from Merck Millipore (Billerica, MA, USA) and alexa flour 488 goat anti-rabbit IgG was purchased from Invitrogen (Carlsbad, CA, USA).

2.2 Formulation of PLGA microspheres

Porous PLGA microspheres were prepared using the double emulsion solvent evaporation method as described in detail elsewhere (Qutachi et al., 2014; Boukari et al., 2015). Briefly, a 250-µl aliquot of PBS was added to a 20% w/v PLGA/DCM solution and homogenized at 9000 rpm using a Silverson L5M homogeniser (East Longmeadow, MA, USA). This was added to 200 ml of 0.3% w/v PVA solution and homogenized at 4000 rpm and then stirred at 300 rpm for 4 hours. The microspheres were washed with distilled water and then exposed to ethanolic-NaOH in order to enhance the surface porosity. They were then sieved (40 µm) and washed using distilled water. Non-porous microspheres were prepared in a similar way using 100 µl of 100 mg/ml BSA solution or 100 µl of distilled water, instead of 250 µl of PBS. BSA was chosen as a model protein as it is compatible with chitosan and has previously been used as a substitute for growth factors (Song et al., 2013; Yilgor et al., 2010; Yilgor et al.,2009).

Non-porous PLGA/chitosan composite microspheres were prepared similarly; however, instead of using 200 ml of 0.3% w/v PVA solution, the aqueous phase comprised 150 ml of 0.4% w/v PVA solution containing 0.05 g of TPP. The primary emulsion, in addition to 50 ml of 0.25% w/v chitosan solution in 2% v/v acetic acid, was added to the external aqueous phase simultaneously and homogenized. All microspheres were freeze-dried using a Thermo Fisher Scientific FR-Drying Digital Unit (Waltham, MA, USA) for 48 hours and stored at -20ºC until use.

2.3 Scanning electron microscopy (SEM) and size analysis

The freeze-dried samples were mounted onto aluminium stubs (Agar Scientific, UK) and gold-coated using a Balzers SCD030 gold sputter coater (Balzers Union Ltd., Lichtenstein). The morphology and surface topography of the microspheres were observed using a Jeol 6060L SEM imaging system (Jeol Ltd., Hertfordshire, UK) at 10 kV. The particle size distribution and mean microsphere diameter were determined using a Coulter LS230 particle size analyser (Beckman, UK).

2.4 Fourier transform infrared (FTIR) spectroscopy

FTIR spectra of the microspheres and their constituents were obtained using a Spectrum RX 1 FTIR spectrophotometer (Perkin Elmer, Waltham, MA, USA). Samples were mixed with potassium bromide (KBr) and compressed using a 5-tonne force into disks; 256 scans were acquired from 400 to 4000 cm^{-1}.

2.5 Preparation of 3D scaffolds

PLGA and PLGA/chitosan composite scaffolds were previously prepared in our laboratories (Boukari et al., 2015). A 1:1 mass ratio of porous to non-porous microspheres was mixed in a weighing boat followed by mixing with PBS (pH 7.4) at a ratio of 0.25:1 (PBS to microspheres) to form a paste. The paste was packed into a 6-mm diameter and 12-mm height polytetrafluorethylene (PTFE) mould using a spatula, and then stored in a sealed de-humidifying chamber at 37°C for 17 hours.

2.6 Time of flight secondary ion mass spectrometry (ToF-SIMS)

The presence and distribution of the chitosan coating on the scaffold surfaces was assessed using a time of flight secondary ion mass spectrometer (ToF-SIMS IV, ION-TOF GmbH, Munster, Germany). Scaffolds were placed on the ToF-SIMS stage and secured with metal clips. A 25-keV Bi_3^+ primary ion source was used to scan a 256 × 256 pixel raster, while simultaneously not exceeding the limit of static, as described by Rafati et al., (2012). Surface charge due to the primary ion beam on the insulating sample surface was compensated using a flood gun generating low energy electrons (20 eV). Negative and positive polarity data for 500 × 500 µm areas were analysed using the SurfaceLab 6 software (IONTOF, Germany). PLGA was identified by the presence of $C_3H_3O_2^-$ (m/z = 71) and $C_3H_5O_2^-$ (m/z = 73) (Rafato et al., 2012). Diagnostic secondary ion peaks for chitosan were identified as CN^- (m/z = 26) from the negative polarity data, in addition to CH_4N^+ (m/z = 30) and $C_4H_5N_2^+$ (m/z = 81) from the positive polarity data. For a semi-quantitative analysis, each area was split into four regions of interest, and the ion intensity data for these peaks of interest were exported and normalized to the total ion intensity.

2.7 Encapsulation efficiency (%EE) of BSA within microspheres and scaffolds

The %EE of BSA within the non-porous PLGA and PLGA/chitosan composite microspheres and scaffolds were determined by gently stirring 10 mg of the microspheres or one scaffold in 750 µl or 13 ml of DMSO, respectively, for 1 hour. This was followed by the addition of 2.15 ml or 37.27 ml of 0.02% w/v SDS in 0.2 M NaOH to the microspheres or scaffolds, respectively. The solution was left to stand at room temperature for 1 hour. Standard concentrations of BSA were calibrated with a BCA reagent so that the sample absorbance could be matched with standard concentrations on an Infinite 200 plate reader (Tecan, Switzerland) at 562 nm. The %EE of BSA within the microspheres and scaffolds was then calculated using Equation 1.

$$\%EE = \frac{\text{Actual mass of BSA in 10mg of microspheres OR 1 scaffold}}{\text{Theoretical mass of BSA used for 10 mg of microspheres OR 1 scaffold}} \times 100 \quad (1)$$

2.8 Release of BSA from microspheres and scaffolds

Release studies of BSA from the PLGA and PLGA/chitosan composite microspheres were carried out by submerging 50 mg of microspheres in 1.5 ml of PBS in a micro-centrifuge tube. The tubes were incubated at 37°C. At predetermined time intervals, the PBS supernatant was removed and replaced with fresh buffer. Aliquots (150 µl) were withdrawn from the supernatant and assayed for the presence of BSA at 562 nm on the microplate reader using the BCA assay kit. BSA release from scaffolds was studied in 4 ml of PBS and assayed as described above.

2.9 Preparation of 3D scaffolds post-injection

Microsphere mixtures were prepared at a 1:1 ratio of porous to non-porous microspheres and an approximate BSA loading of 3 mg of BSA/g of mixture, as described in section 2.5. The mixture was suspended in PBS at a concentration of 50 mg of microspheres/ml, vortex-mixed briefly and then drawn into a 1-ml syringe (BD Fine) fitted with a 19-G needle (1.1 × 50 mm, BD fine, Franklin Lakes, NJ, USA). Finally, the contents of the syringe were injected into the PTFE scaffold mould.

2.10 Compressive strength of scaffolds

The compressive strength of the scaffolds was assessed using a TA.HD+ texture analyser (Stable Microsystems, UK) equipped with a 50-kg load cell at a speed of 0.04

mm/second over a contact area of approximately 28.75 mm^2. Dry PLGA and PLGA/chitosan BSA-loaded scaffolds prepared as described in sections 2.5 and 2.9 were tested, and the compressive strength was determined as the stress at the maximum strain.

2.11 Cell culture and seeding onto scaffolds

Primary hMSCs were cultured in hMSC basal media supplemented with the contents of an MSCGM hMSC SingleQuot kit. The cells were maintained in a humidified tissue-culture incubator at 37°C in 5% CO_2. The cytocompatibility test was carried out on BSA-free scaffolds. Scaffolds were prepared directly into a 24-well plate in a manner similar to that described in section 2.5. A 1:1 porous to non-porous microsphere mixture was UV sterilised for 80 minutes (Gould et al., 2013) and then transferred to the well. Basal growth medium was then added at a ratio of 0.25:1 (medium to microspheres). After 17 hours of sintering, each scaffold was seeded with 1×10^5 hMSCs and incubated for 2 hours, followed by the addition of 1 ml of media to each scaffold/well. The cell-seeded scaffolds were maintained at 37°C with 5% CO_2. For all cell experiments, either 5 replicates or 2 independent repeats each comprising at least 3 replicates was carried out.

2.12 Cell viability assay

Each scaffold was submerged in 1 ml of media and 111 µl of Presto Blue reagent and the cell viability was determined at day 1, 3, 6 and 8 post-seeding using the Presto Blue cell viability reagent. The well plate was protected from light and incubated at 37°C for 25 minutes. Aliquots of 100 µl were withdrawn from each well in triplicate and the absorbance was read on an infinite 200 plate reader (Tecan, Switzerland) at excitation and emission wavelengths of 560 nm and 590 nm, respectively. The Presto Blue reagent was replaced with fresh media and the scaffolds were placed back in the incubator. On day 8, after measuring the cell viability, the scaffolds were washed with PBS and the cells were fixed with 10% v/v buffered formalin solution for 20 minutes. Fixed hMSC-scaffold constructs were viewed under the SEM.

2.13 Assessment of mineralization

In order to determine the degree of mineralization on the scaffolds, the von Kossa assay was utilized. Cells were seeded onto scaffolds as described in section 2.11 and incubated in basal growth media for 21 days. On day 21, cells were fixed with 10% v/v buffered formalin for 20 minutes and thoroughly washed with PBS. A 450-µl aliquot of 1% w/v silver nitrate solution was added to each scaffold and incubated under a UV light source for 1 hour. The solution was then removed and the scaffolds were washed three times with deionized water. This was followed by treatment with sodium thiosulphate solution for 5 minutes in order to remove any excess silver nitrate solution. The scaffolds were then washed with PBS prior to imaging under a dissection microscope (Leica, Germany).

2.14 Osteocalcin immunostaining

Cells were seeded onto scaffolds as described in section 2.11. The scaffolds were incubated in basal growth media for 21 days after which they were fixed using 10% v/v paraformaldehyde for 20 minutes and then thoroughly washed with PBS. The cells were permeabilised with 500 µl of 0.1% v/v Triton X-100 solution for 40 minutes. The solution was aspirated and the cells were washed with PBS. Blocking of unspecific binding sites as a result of epitomes on the cell layers was carried out via the addition of 500 µl of 3% v/v goat serum in 1% w/v BSA in PBS for 40 minutes. The blocking solution was removed and 500 µl of anti-OCN primary antibody solution (1:200 dilution in 1% w/v BSA in PBS) was added. The scaffolds were incubated at 4°C overnight. After incubation, the antibody solution was removed, the scaffolds were washed with PBS and then incubated at room temperature for two hours in 500 µl of a 1:200 solution of Alexa Flour 488 goat anti-rabbit secondary IgG, in 1% w/v BSA in PBS. After incubation, the secondary antibody solution was removed and the scaffolds were washed with PBS. In order to stain the DNA of cells, the scaffolds were incubated for a further 15 minutes in 1 µg/ml Hoechst dye dissolved in 1% w/v BSA in PBS at room temperature. After incubation, the Hoechst dye was removed and the scaffolds were thoroughly washed with PBS and then viewed under a dissection microscope. The images of PLGA and composite scaffolds were processed and compared using the ImageJ software (Version 1.48, National Institute of Health, Bethesda, MD, USA). Four images were taken of four different areas on each scaffold and then converted into binary formats so that the stained areas could be calculated.

2.15 Statistical Analyses

A statistical analysis of the data was carried out using Microsoft Excel. An unpaired t test and the ANOVA procedure were used and the results were deemed significant when $p < 0.05$.

3. Results

3.1 Physical characterization of PLGA/chitosan composite microspheres and scaffolds

BSA-encapsulated PLGA/chitosan composite microspheres were formulated using TPP as a cross-linker as detailed in section 2.2. Both the PLGA and composite microspheres appeared smooth, as shown in the SEM images in Figure 1A and B, respectively. Thus, the addition of chitosan cross-linked with TPP did not alter the superficial appearance of the microspheres and no unprocessed, free chitosan is visible from the SEM images. Size analysis revealed the average diameters of the PLGA and composite microspheres to be 69.75 ± 21.47 µm and 66.85 ± 22.68 µm, respectively (Figure 1C).

The FTIR spectra of the raw materials and microspheres are presented in Figure 2. The chitosan spectrum shows a high-intensity peak at 3400 cm^{-1}, which corresponds to stretching vibrations of the O-H and N-H bonds, in addition to hydrogen bonding in the backbone (Azevedo et al., 2011). The characteristic peak at 1647 cm^{-1} is a result of the amide functionality and may be present as a consequence of the axial deformation of the C=O bond (Azevedo et al., 2011) and strong N-H bending (Misch et al., 1999). Peaks present at 1019 and 1086 cm^{-1} (corresponding to C-O stretch vibrations), and 1152 cm^{-1} (asymmetric stretch of the C-O-C bond) are also indicative of chitosan (Azevedo et al., 2011).

The TPP spectrum, similarly, shows a peak of significant intensity at 3390 cm^{-1}, corresponding to the stretching vibrations of the O-H bond. Peaks around the 1095 cm^{-1} region are an indication of the P=O phosphate group. The PLGA spectrum presents a peak at 3473 cm^{-1}, which is indicative of vibration of the terminal O-H groups. Other peaks that indicate PLGA are present at 743 cm^{-1} (C-H bend), 1086 and 1180 cm^{-1} (C-O stretch), 1381 cm^{-1} (C-H bend), 1771 cm^{-1} (the carbonyl C=O) and 2876 cm^{-1} (CH_2 bend) (Ganji and Abdekhodaie, 2010). Both PLGA and PLGA/chitosan composite BSA-loaded microspheres show peaks at identical wavelengths, which suggests that the microspheres are predominantly PLGA. Moreover, the spectra of PLGA and PLGA/chitosan composite microspheres show peaks at 1621 cm^{-1} and 1639 cm^{-1}, respectively, which are attributed to the C=O bond of the amide groups that are found both in BSA and chitosan. However, there does appear to be a slightly more pronounced peak at 1639 cm^{-1} on the spectrum of the PLGA/chitosan composite microspheres, which corresponds to the amide C=O bond suggesting the presence of chitosan in the formulation.

The ToF-SIMS analysis was carried out in order to ascertain the presence of chitosan on the scaffold surfaces. BSA-free scaffolds were analysed based on the overlap of chitosan and BSA secondary ion peaks (discussed in section 2.6). Intensities of nitrogen-containing positive secondary ion peaks CH_4N^+ ($m/z = 30$) and $C_4H_5N_2^+$ ($m/z = 81$), as well as the negative ion peak CN^- ($m/z = 26$) were all significantly higher in the composite PLGA/chitosan scaffolds when compared to the chitosan-free scaffolds, as shown in Figure 3A. However, there was no significant difference between the profiles of diagnostic PLGA ion peaks for the PLGA and composite scaffolds (Figure 3B).

The incorporation of chitosan did not elicit a significant change in the encapsulation efficiency of BSA in the microspheres, with 80.58 ± 17.06% and 81.57 ± 3.06% of the protein being encapsulated into the PLGA and PLGA/chitosan composite microspheres, respectively. Moreover, there was no statistical difference in the encapsulation efficiencies of the PLGA and composite scaffolds (2.81 mg/g [93.68% ± 3.50%] and 2.52 mg/g [84.02% ± 12.08%] for the PLGA and PLGA/chitosan composite scaffolds, respectively).

3.2 Release of BSA from microspheres and scaffolds

The release profile of BSA was mapped over 28 days from both microspheres and scaffolds sintered at 37°C (Figure 4). The initial burst release after 24 hours from the PLGA microspheres was significantly higher than from the PLGA/chitosan composite microspheres, 0.93 ± 0.06 µg/mg and 0.57 ± 0.03 µg/mg, respectively ($p < 0.05$). After 28 days, 1.72 ± 0.23 µg/mg of BSA was released from the PLGA microspheres, which was ~~significantly~~ higher in comparison to 1.20 ± 0.05 µg/mg from the PLGA/chitosan composite microspheres ($p = 0.05$)

Similarly, there was a significant retardation of the initial burst release from the scaffolds containing PLGA/chitosan composite microspheres, 0.10 ± 0.02 µg/mg, in comparison to the PLGA scaffolds, 0.16 ± 0.01 µg/mg ($p < 0.05$, Figure 4B).

3.3 Sintering of microspheres into scaffolds

In order to study the effect of the scaffold preparation method on their subsequent morphology and mechanical strength, the PLGA and PLGA/chitosan composite scaffolds were prepared using two different methods. Firstly, a paste was formed from the microspheres as previously reported (Boukari et al., 2015). In the second method, we aimed to study the ability of the microspheres to sinter post-injection through a 19-G needle into a scaffold mould. This was then followed by a 17-hour incubation period at 37°C. Photographs of the resulting scaffolds and their compressive strengths are presented in Figure 5A and B, respectively. The sintering process results in the expulsion of water so that the components within close proximity. We believe that this favours ‘fusion’ and bond formation within the scaffolds. This approach to scaffold sintering at 37^{o}C is superior to the more harsh methods employing elevated temperatures and reagents.

The overall appearances of PLGA and composite scaffolds were very similar (Figure 5A). However, when comparing scaffolds prepared using the paste method, the compressive strength of PLGA/chitosan composite scaffolds was significantly higher (0.846 ± 0.272 MPa) than the PLGA scaffolds (0.406 ± 0.265 MPa, $p < 0.05$).

Figure 5A shows that it was possible to successfully sinter a microsphere suspension post-injection, thus, forming intact scaffolds that retained their shape when removed from the mould. This confirms the injectable potential of the microspheres. When scaffolds were sintered as a suspension post-injection, there was no significant difference between the compressive strengths of the PLGA and PLGA/chitosan composite scaffolds, 0.086 ± 0.068 MPa and 0.048 ± 0.00096 MPa, respectively ($p > 0.05$, Figure 5B); however, it is likely that the compressive values may be below the lower limit of threshold of the machine.

3.4 Cell proliferation on scaffolds

The culturing of primary hMSCs on the scaffolds was used as a means to test their cytocompatibility. Cell proliferation was assessed using the Presto Blue viability reagent on day 1, 3, 6 and 8 (Figure 6A).

Cell proliferation increased over time on both scaffold types. On day 1, the cell numbers on PLGA and PLGA/chitosan composite scaffolds were 1.06×10^4 and 1.03×10^4, respectively. Both types of scaffolds exhibited a very similar cell growth profile with no statistically significant difference found between them ($p > 0.05$) on day 1, 3 and 6. However, the cell number on day 8 was significantly higher on the PLGA scaffolds ($p < 0.05$) at 6.25×10^4 and 4.45×10^4 for PLGA and PLGA/chitosan composite scaffolds, respectively. SEM images of the cell-scaffold constructs on day 8 are shown in Figure 6B and C, with cells visibly distributed between microspheres in both scaffold types.

3.5 Assessment of mineralization

The extent of mineralization on the scaffolds after 21 days in culture media was assessed using the von Kossa assay as described in section 2.14. Dark brown/black nodules (indicated by the white arrow in Figure 7B) are visible on the scaffolds and represent positive staining. A qualitative analysis shows that there are more nodules on the PLGA/chitosan composite scaffolds (Figure 7B), which appear darker in the figure, in comparison to the PLGA scaffolds (Figure 7A).

3.6 Osteocalcin immunostaining

The presence of the bone marker protein, osteocalcin, was detected using the immunostaining technique described in section 2.14. The data obtained was processed using ImageJ, which allowed us to quantify the amount of stain present on each scaffold. The results of this analysis show that there was an increase in osteocalcin staining on the composite scaffolds when compared to the PLGA scaffolds ($p < 0.05$, Figure 8A). When osteogenic media was used (data not shown), the osteocalcin staining on the PLGA/chitosan and PLGA scaffolds was not significantly different ($p > 0.05$). Processed, merged images are shown in Figure 8B and C, with osteocalcin represented in green, and cell DNA in blue.

4. Discussion

Scaffolds made from biodegradable microspheres are a promising approach for bone regeneration. However, there are several features to consider when developing such systems. These include the incorporation of porosity and growth factors into the scaffolds, whilst at the same time providing mechanical strength to enable the microspheres to be injectable and sinter *in situ*. Some research groups have developed scaffolds with some of these properties; however, most groups do not take into account all desirable features in one system. In the present study, we propose a novel dual-application PLGA/chitosan composite scaffold system with the potential to meet all of the above desirable criteria. The system comprises porous and non-porous protein-loaded microspheres with the ability to sinter at 37°C and release protein. The mechanical strength of the system is dependent upon its mode of application, with a higher compressive strength achievable when it is applied as a paste, and sufficient strength to maintain the shape (as evident from the fact that the microspheres sintered at 37°C and were subsequently removed from the mould intact) when injected as a suspension. The cytocompatibility and osteogenic potential of the formulation were evaluated and compared with our previously reported system (Boukari et al., 2015).

Protein-loaded microspheres were formulated using PLGA and chitosan, where the chitosan was cross-linked using TPP. There were no observable differences in the morphology and size of the composite microspheres when compared with PLGA microspheres. The presence of chitosan within the composite scaffolds formed via the paste method was confirmed by ToF-SIMS, suggests that chitosan is formed as part of the microstructure of the particles. Furthermore, the composite scaffolds demonstrated higher compressive strength than the PLGA scaffolds. In this regard, chitosan contributes to the mechanical strength of the scaffolds, due to interactions between the negatively charged PLGA (Balmert et al., 2015) and the protonated amine groups in the chitosan structure. Moreover, the compressive strength demonstrated by the composite scaffolds fell within an acceptable range as reported by Misch et al. (1999).

The chitosan coating attenuated the initial burst release from the microspheres and scaffolds, and this reduction may partly be attributed to chitosan complexing with BSA (isoelectric point, approximately 5), thereby, impeding its release. The ability of chitosan, a natural polyelectrolyte, to non-covalently bind to negatively charged proteins has been reported (Boeris et al., 2010). A similar observation of a reduced burst release was made for the same system when encapsulated with lysozyme, which is positively charged at a neutral pH (data not shown). This suggests that other factors contribute to the reduction in burst release. It has been reported that the burst release of proteins from PLGA microspheres is usually due to protein residing near, or on the surface of, the delivery system (Zeng and Liang, 2010). We believe that the formation of a chitosan -TPP matrix layer slows the release of the protein and significantly contributes to the attenuation in the initial burst release. This effect has been demonstrated in PLGA/chitosan microspheres encapsulated with a non-protein drug, rifampicin, in which the addition of chitosan caused a reduction in the burst release (Manca et al., 2008). The slower, steadier release of BSA from the microspheres and scaffolds containing PLGA/chitosan is desirable in BMP-2 applications. The controlled release reduces the need for supra-physiological loadings, which are necessary when there is a huge initial loss via a burst release (Kirby et al., 2011).

The system described herein possesses dual-applicability arising from the formulation's potential of having two application modes (i) a paste that is implanted within a degenerated bone tissue, takes the shape of the defect area and then sinters at 37°C, and (ii) the injection of the microsphere suspension directly into the defect area. The former would be useful in applications requiring a relatively stronger scaffold, such as the regeneration of cancellous bone for which the ultimate compressive strength has been reported to range from 0.22 to 10.44 MPa (Misch et al., 1999). However, the latter is more suited to applications in which the delivery system may be injected and remain in one location, hence, allowing the controlled delivery of a specific, known dose of protein to the site. To our knowledge, this is the first time that the ability of microspheres to sinter at 37°C, post-injection, has been demonstrated.

The ability of cells to attach and grow on the scaffolds is paramount in the development of protein delivery systems in regenerative medicine. For this reason, the cytocompatibility of the scaffolds with hMSCs was investigated. The cell number increased on the composite scaffolds over the 8-day period from 1.03×10^4 on day 1, to 4.45×10^4 on day 8. There was no significant difference between cell numbers on the composite and PLGA scaffolds, except on day 8, by which time the cell numbers were higher on PLGA scaffolds ($p < 0.05$). Although previous studies have investigated the cytocompatibility of sintered composite PLGA/chitosan microspheres scaffolds with other cell types, these formulations were not capable of sintering *in situ* (Tao et al., 2014).

The potential of the scaffold material to promote the differentiation of hMSCs is another key factor that is crucial for the production of a successful biomaterial. Although the presence of BMP-2 has been shown to promote osteogenic differentiation, the intrinsic ability of the material itself to promote the process is also of interest. Chitosan has been reported to have numerous biomedical properties, including its ability to improve osteogenesis in animal bone defect models (Lee et al., 2008). In this study, we investigated the cell response to protein-free scaffolds in basal media in order to study the effect of the scaffold material on osteogenesis. The presence of a calcified ECM is a reliable way of confirming osteogenesis (Declercq et al., 2005). Nodules were observed on both composite and PLGA scaffolds based on von Kossa staining, which indicates the presence of calcium. To provide further confirmation of the deposition of a calcified matrix, the presence of osteocalcin, a late protein marker of osteogenic differentiation, was determined. Its expression is known to rise with an increase in mineralization (Stein et al., (1990). The composite scaffolds showed a significantly higher degree of osteocalcin staining when compared to the PLGA scaffolds. Previous studies have demonstrated the ability of chitosan-containing scaffolds to induce differentiation in the presence of osteogenic media (Jiang et al., 2006), which we also confirmed (data not shown). However, relatively little evidence has demonstrated this in basal growth media. Therefore, these results suggest that the inclusion of chitosan in PLGA microspheres enhanced the osteogenic capacity of the resultant scaffolds.

5. Conclusion

In this study, a novel, dual-application composite microsphere system was developed with the ability to fuse together as a paste, thereby forming an intact scaffold in the body at

37°C. Furthermore, the ability of a suspension of the microspheres to sinter post-injection was also demonstrated. Composite PLGA/chitosan microspheres were shown to attenuate the initial burst release and elicited a steady, slow release of protein over 28 days. The scaffold's cytocompatibility and ability to promote osteogenesis were also demonstrated. This technology, therefore, exhibits potential as a scaffold for bone regeneration and is an excellent candidate for further *in vitro* and *in vivo* testing.

Disclosures

There are no potential conflicts of interest to disclose for this work.

Acknowledgements

This work was funded by the European Community under the FP7 project 519 Biodesign EUFP7-NMP.20102.3-1. The authors would also like to thank Enas Alkhader, Hilda Amekyeh, Abdulrahman Baki and Noura Alom (The University of Nottingham) for their support and assistance.

This article contains supplementary material available from the authors upon request or via the Internet at http://wileylibrary.com.

References:

Amini AR, Laurencin CT, Nukavarapu SP 2012. Bone Tissue Engineering: Recent Advances and Challenges. Crit Rev Biomed Eng 40: 363–408.

Azevedo JR, Sizilio RH, Brito MB, Costa a. MB, Serafini MR, Araújo a. a S, et al. 2011. Physical and chemical characterization insulin-loaded chitosan-TPP nanoparticles. J Therm Anal Calorim 106: 685–689.

Balmert SC, Zmolek AC, Glowacki AJ, Knab TD, Rothstein SN, Wokpetah JM, et al. 2015. Positive charge of “sticky” peptides and proteins impedes release from negatively charged PLGA matrices. J Mater Chem B 3: 4723–4734.

Boeris V, Farruggia B, Pico G 2010. Chitosan-bovine serum albumin complex formation: A model to design an enzyme isolation method by polyelectrolyte precipitation. J Chromatogr B-Analytical Technol Biomed Life Sci 878: 1543–1548.

Bostrom R, Mikos AG 1997. Tissue Engineering of Bone, in: Synth. Biodegrad. Polmer Scaffolds, : pp. 215–234.

Boukari Y, Scurr DJ, Qutachi O, Morris AP, Doughty SP, Rahman C V, Billa N 2015. Physicomechanical properties of sintered scaffolds formed from porous and protein-loaded poly(DL-lactic-co-glycolic acid) microspheres for potential use in bone tissue engineering. J Biomater Sci Polym Ed 26: 796–811.

Burg KJ, Porter S, Kellam JF 2000. Biomaterial developments for bone tissue engineering. Biomaterials 21: 2347–2359.

Casettari L, Castagnino E, Stolnik S, Lewis A, Howdle SM, Illum L 2011. Surface characterisation of bioadhesive PLGA/chitosan microparticles produced by supercritical fluid technology. Pharm Res 28: 1668–1682.

Chakravarthi SS, Robinson DH 2011. Enhanced cellular association of paclitaxel delivered in chitosan-PLGA particles. Int J Pharm 409: 111–120.

Chen FM, Zhang M, Wu ZF 2010. Toward delivery of multiple growth factors in tissue engineering. Biomaterials 31: 6279–6308.

Choi DH, Subbiah R, Kim IH, Han DK, Park K 2013. Dual growth factor delivery using biocompatible core-shell microcapsules for angiogenesis. Small 9: 3468–3476.

Declercq H, Verbeeck R, Deridder L, Schacht E, Cornelissen M 2005. Calcification as an indicator of osteoinductive capacity of biomaterials in osteoblastic cell cultures. Biomaterials 26: 4964–4974.

Delloye C, Cornu O, Druez V, Barbier O 2007. Bone allografts: What they can offer and what they cannot. J Bone Joint Surg Br 89: 574–579.

Dhillon A, Schneider P, Kuhn G, Reinwald Y, White LJ, Levchuk A, et al. 2011. Analysis of sintered polymer scaffolds using concomitant synchrotron computed tomography and in situ mechanical testing. J Mater Sci Mater Med 22: 2599–2605.

Di Martino A, Sittinger M, Risbud M V. 2005. Chitosan: A versatile biopolymer for orthopaedic tissue-engineering. Biomaterials 26: 5983–5990.

Fu Y, Du L, Wang Q, Liao W, Jin Y, Dong A, et al. 2012. In vitro sustained release of recombinant human bone morphogenetic protein-2 microspheres embedded in thermosensitive hydrogels. Pharmazie 67: 299–303.

Ganji F, Abdekhodaie MJ 2010. Chitosan-g-PLGA copolymer as a thermosensitive membrane. Carbohydr Polym 80: 740–746.

Gould TW a, Birchall JP, Mallick AS, Alliston T, Lustig LR, Shakesheff KM, Rahman C V 2013. Development of a porous poly(DL-lactic acid-co-glycolic acid)-based scaffold for mastoid air-cell regeneration. Laryngoscope 123: 3156–3161.

Han F, Zhou F, Yang X, Zhao J, Zhao Y, Yuan X 2015. Facile Preparation of PLGA Microspheres With Diverse Internal Structure by Modified Double-Emulsion Method for Controlled Release. Polym Eng Sci 55: 896–906.

Hsu WK, Wang JC 2008. Contemporary concepts in spine care- the use of bone morphogenetic protein in spine fusion. Spine J 8: 419–425.

Hu X, Zhou J, Zhang N, Tan H, Gao C 2008. Preparation and properties of an injectable scaffold of poly(lactic-co-glycolic acid) microparticles/chitosan hydrogel. J Mech Behav Biomed Mater 1: 352–359.

Jaklenec A, Hinckfuss A, Bilgen B, Ciombor DM, Aaron R, Mathiowitz E 2008. Sequential release of bioactive IGF-I and TGF-β1 from PLGA microsphere-based scaffolds. Biomaterials 29: 1518–1525.

Jaklenec A, Wan E, Murray ME, Mathiowitz E 2008. Novel scaffolds fabricated from protein-loaded microspheres for tissue engineering. Biomaterials 29: 185–192.

Jiang T, Abdel-Fattah WI, Laurencin CT 2006. In vitro evaluation of chitosan/poly(lactic acid-glycolic acid) sintered microsphere scaffolds for bone tissue engineering. Biomaterials 27: 4894–4903.

Jiang T, Khan Y, Nair LS, Abdel-Fattah WI, Laurencin CT 2010. Functionalization of chitosan/poly(lactic acid-glycolic acid) sintered microsphere scaffolds via surface heparinization for bone tissue engineering. J Biomed Mater Res A 93: 1193–1208.

Jiang T, Nukavarapu SP, Deng M, Jabbarzadeh E, Kofron MD, Doty SB, et al. 2010. Chitosan-poly(lactide-co-glycolide) microsphere-based scaffolds for bone tissue engineering: In vitro degradation and in vivo bone regeneration studies. Acta Biomater 6: 3457–3470.

Kirby GTS, White LJ, Rahman C V., Cox HC, Qutachi O, Rose FRAJ, et al. 2011. PLGA-Based Microparticles for the Sustained Release of BMP-2. Polymers (Basel) 3: 571–586.

Lee J-Y, Nam S-H, Im S-Y, Park Y-J, Lee Y-M, Seol Y-J, et al. 2002. Enhanced bone formation by controlled growth factor delivery from chitosan-based biomaterials. J Control Release 78: 187–197.

Lu JM, Wang X, Marin-Muller C, Wang H, Lin PH, Yao Q, Chen C 2009. Current advances in research and clinical applications of PLGA based nanotechnology. Expert Rev Mol Diagn 9: 325–341.

Luciani A, Coccoli V, Orsi S, Ambrosio L, Netti P a. 2008. PCL microspheres based functional scaffolds by bottom-up approach with predefined microstructural properties and release profiles. Biomaterials 29: 4800–4807.

Makadia HK, Siegel SJ 2011. Poly Lactic-co-Glycolic Acid (PLGA) as Biodegradable Controlled Drug Delivery Carrier. Polymers (Basel) 3: 1377–1397.

Manca ML, Loy G, Zaru M, Fadda AM, Antimisiaris SG 2008. Release of rifampicin from chitosan, PLGA and chitosan-coated PLGA microparticles. Colloids Surf B Biointerfaces 67: 166–70.

Martino S, D’Angelo F, Armentano I, Kenny JM, Orlacchio A 2012. Stem cell-biomaterial interactions for regenerative medicine. Biotechnol Adv 30: 338–351.

Misch E, Qu Z, Bidez MW 1999. Mechanical properties of trabecular bone in the human mandible: implications for dental implant treatment planning and surgical placement. J Oral Maxillofac Surg 57: 700–706.

Nauth A, Ristevski B, Li R, Schemitsch EH 2011. Growth factors and bone regeneration: how much bone can we expect? Injury 42: 574–579.

Paillard-Giteau A, Tran VT, Thomas O, Garric X, Coudane J, Marchal S, et al. 2010. Effect of various additives and polymers on lysozyme release from PLGA microspheres prepared by an s/o/w emulsion technique. Eur J Pharm Biopharm 75: 128–136.

Pan Z, Ding J 2012. Poly(lactide-co-glycolide) porous scaffolds for tissue engineering and regenerative medicine. Interface Focus 2: 366–377.

Pan Z, Ding J 2012. Poly(lactide-co-glycolide) porous scaffolds for tissue engineering and regenerative medicine. Interface Focus 2: 366–377.

Pandey CM, Sharma A, Sumana G, Tiwari I, Malhotra BD 2013. Cationic poly(lactic-co-glycolic acid) iron oxide microspheres for nucleic acid detection. Nanoscale 5: 3800–3807.

Patel ZS, Yamamoto M, Ueda H, Tabata Y, Mikos AG 2008. Biodegradable gelatin microparticles as delivery systems for the controlled release of bone morphogenetic protein-2. Acta Biomater 4: 1126–1138.

Puppi D, Chiellini F, Piras a. M, Chiellini E 2010. Polymeric materials for bone and cartilage repair. Prog Polym Sci 35: 403–440.

Qian L, Zhang H 2013. One-step synthesis of protein-encapsulated microspheres in a porous scaffold by freeze-drying double emulsions and tuneable protein release. Chem Commun 49: 8833–8835.

Qutachi O, Vetsch JR, Gill D, Cox H, Scurr DJ, Hofmann S, et al. 2014. Injectable and porous PLGA microspheres that form highly porous scaffolds at body temperature. Acta Biomater 10: 5090–5098.

Rafati A, Boussahel A, Shakesheff KM, Shard AG, Roberts CJ, Chen X, et al. 2012. Chemical and spatial analysis of protein loaded PLGA microspheres for drug delivery applications. J Control Release 162: 321–329.

Song K, Liu Y, Macedo HM, Jiang L, Li C, Mei G, Liu T 2013. Fabrication and evaluation of a sustained-release chitosan-based scaffold embedded with PLGA microspheres. Mater Sci Eng C 33: 1506–1513.

Song K, Liu Y, MacEdo HM, Jiang L, Li C, Mei G, Liu T 2013. Fabrication and evaluation of a sustained-release chitosan-based scaffold embedded with PLGA microspheres. Mater Sci Eng C 33: 1506–1513.

Stein GS, Lian JB, Owen T a 1990. Relationship of cell growth to the regulation of tissue-specific gene expression during oseoblast differentiation. FASEB J 4: 3111–3123.

Tao C, Huang J, Lu Y, Zou H, He X, Chen Y, Zhong Y 2014. Development and characterization of GRGDSPC-modified poly(lactide-co-glycolide acid) porous microspheres incorporated with protein-loaded chitosan microspheres for bone tissue engineering. Colloids Surfaces B Biointerfaces 122: 439–446.

Tran VT, Benoît JP, Venier Julienne MC 2011. Why and how to prepare biodegradable, monodispersed, polymeric microparticles in the field of pharmacy? Int J Pharm 407: 1–11.

Vo TN, Kasper FK, Mikos AG 2012. Strategies for controlled delivery of growth factors and cells for bone regeneration. Adv Drug Deliv Rev 64: 1292–1309.

Wang Y, Shi X, Ren L, Wang C, Wang D-A 2009. Porous poly (lactic-co-glycolide) microsphere sintered scaffolds for tissue repair applications. Mater Sci Eng C 29: 2502–2507.

Wang Y, Shi X, Ren L, Yao Y, Zhang F, Wang D-A 2010. Poly(lactide-co-glycolide)/titania composite microsphere-sintered scaffolds for bone tissue engineering applications. J Biomed Mater Res B Appl Biomater 93: 84–92.

White LJ, Kirby GTS, Cox HC, Qodratnama R, Qutachi O, Rose FRAJ, Shakesheff KM 2013. Accelerating protein release from microparticles for regenerative medicine applications. Mater Sci Eng C Mater Biol Appl 33: 2578–2583.

Yilgor P, Hasirci N, Hasirci V 2010. Sequential BMP-2/BMP-7 delivery from polyester nanocapsules. J Biomed Mater Res - Part A 93: 528–536.

Yilgor P, Tuzlakoglu K, Reis RL, Hasirci N, Hasirci V 2009. Incorporation of a sequential BMP-2/BMP-7 delivery system into chitosan-based scaffolds for bone tissue engineering. Biomaterials 30: 3551–3559.

Yu Y, Chen J, Chen R, Cao L, Tang W, Lin D, et al. 2015. Enhancement of VEGF-Mediated Angiogenesis by 2- *N* ,6- *O* -Sulfated Chitosan-Coated Hierarchical PLGA Scaffolds. ACS Appl Mater Interfaces 7: 9982–9990.

Zeng W, Huang J, Hu X, Xiao W, Rong M, Yuan Z, Luo Z 2011. Ionically cross-linked chitosan microspheres for controlled release of bioactive nerve growth factor. Int J Pharm 421: 283–290.

Zheng C hong, Liang W 2010. A one-step modified method to reduce the burst initial release from PLGA microspheres. Drug Deliv 17: 77–82.

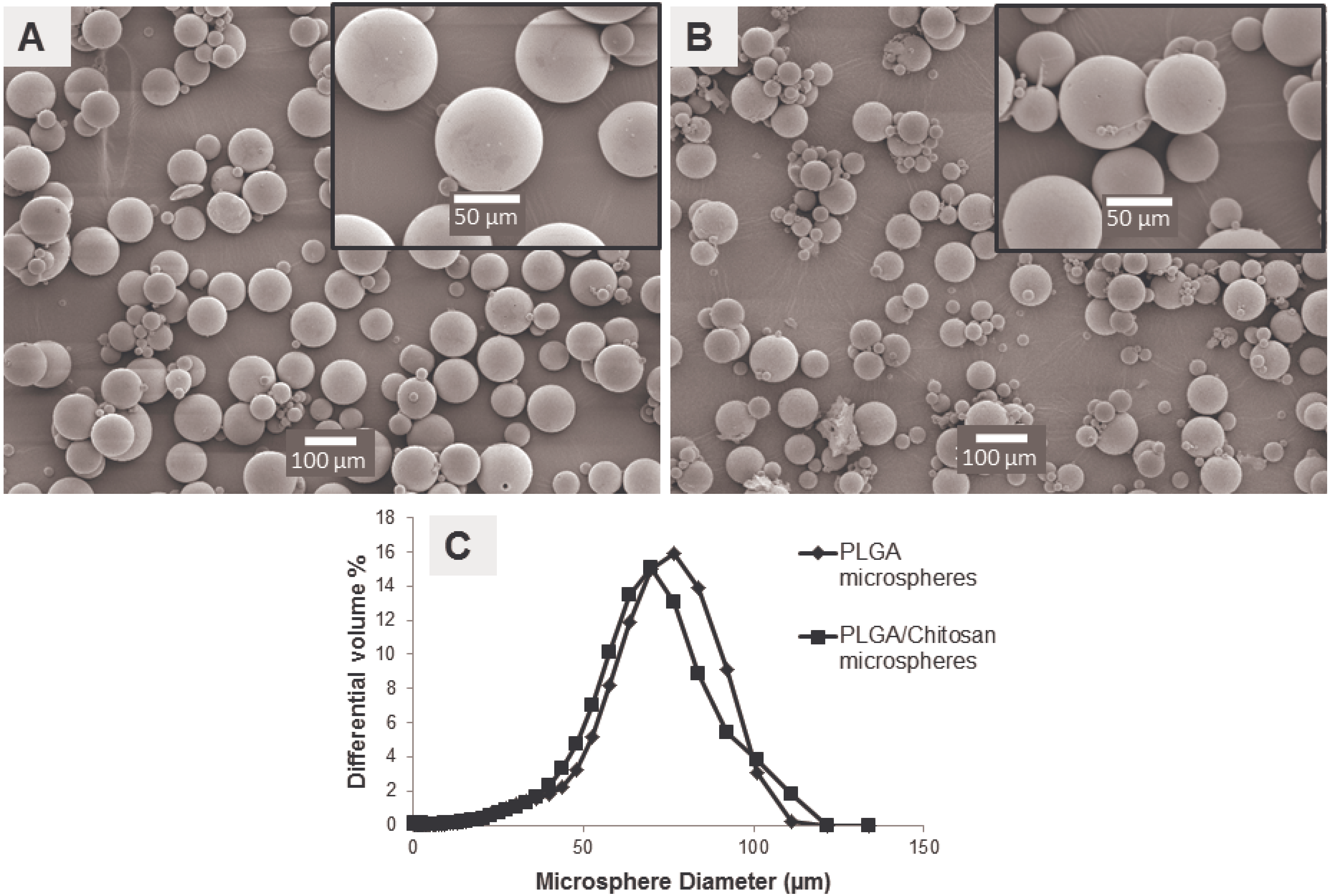

A
50 µm
100 µm
B
50 µm
100 µm
C
Differential volume %
Microsphere Diameter (µm)
PLGA microspheres
PLGA/Chitosan microspheres
0
2
4
6
8
10
12
14
16
18
0
50
100
150

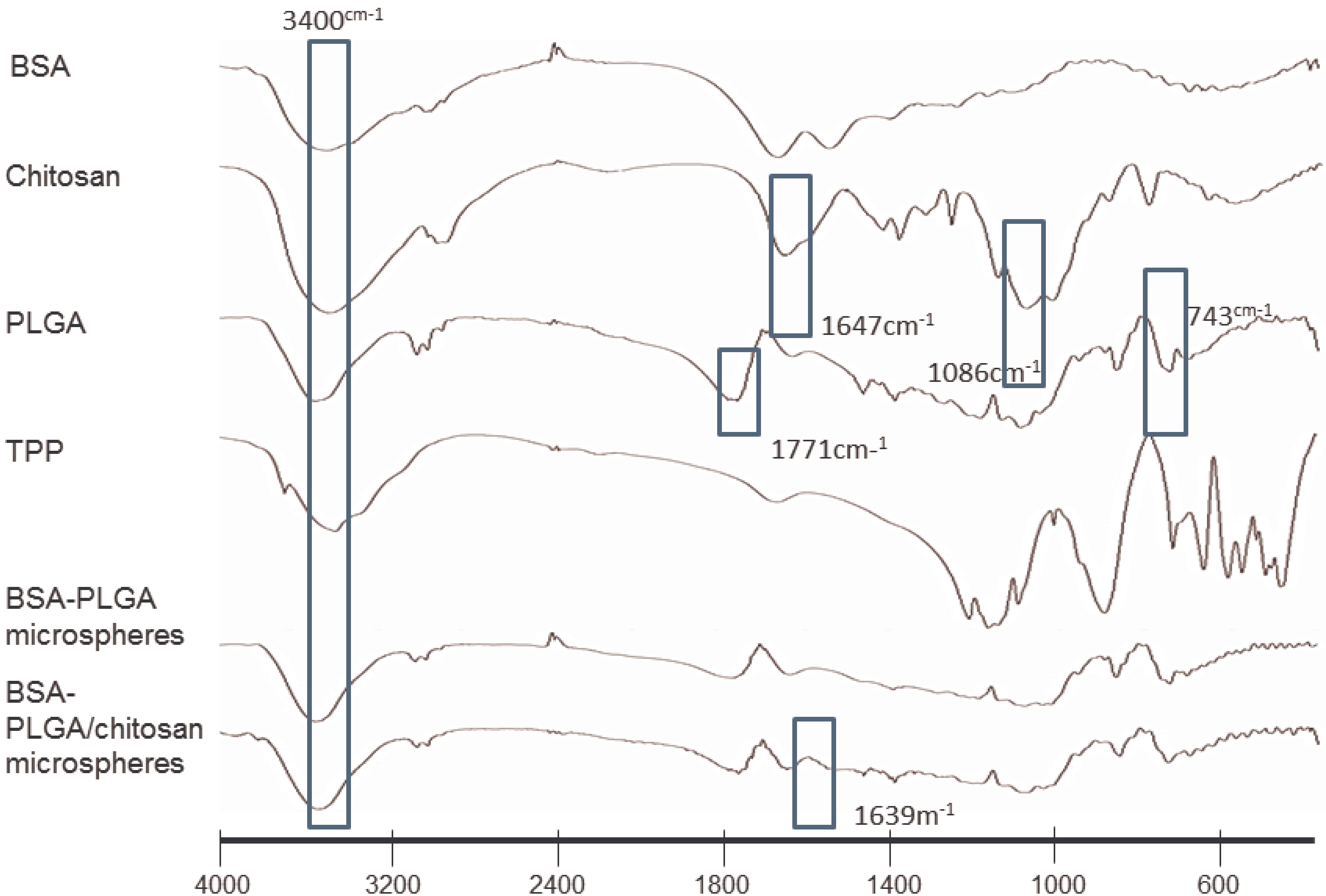

3400cm-1
BSA
Chitosan
PLGA
TPP
BSA-PLGA microspheres
BSA-PLGA/chitosan microspheres
1647cm-1
1086cm-1
743cm-1
1771cm-1
1639m-1
4000
3200
2400
1800
1400
1000
600

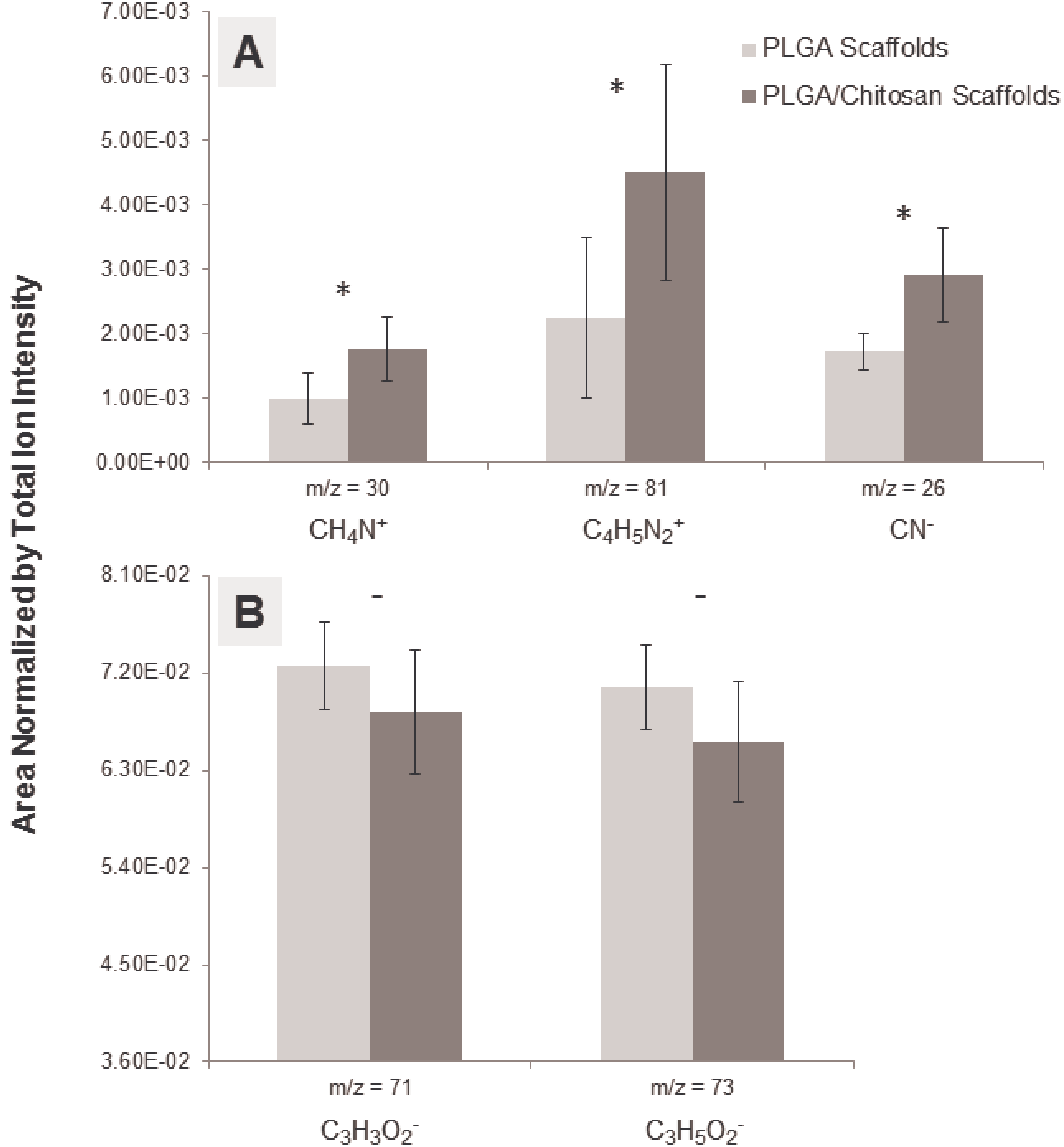
A
B
PLGA Scaffolds
PLGA/Chitosan Scaffolds
Area Normalized by Total Ion Intensity
7.00E-03
6.00E-03
5.00E-03
4.00E-03
3.00E-03
2.00E-03
1.00E-03
0.00E+00
m/z = 30
CH_4N^+
m/z = 81
$C_4H_5N_2^+$
m/z = 26
CN^-
8.10E-02
7.20E-02
6.30E-02
5.40E-02
4.50E-02
3.60E-02
m/z = 71
$C_3H_3O_2^-$
m/z = 73
$C_3H_5O_2^-$

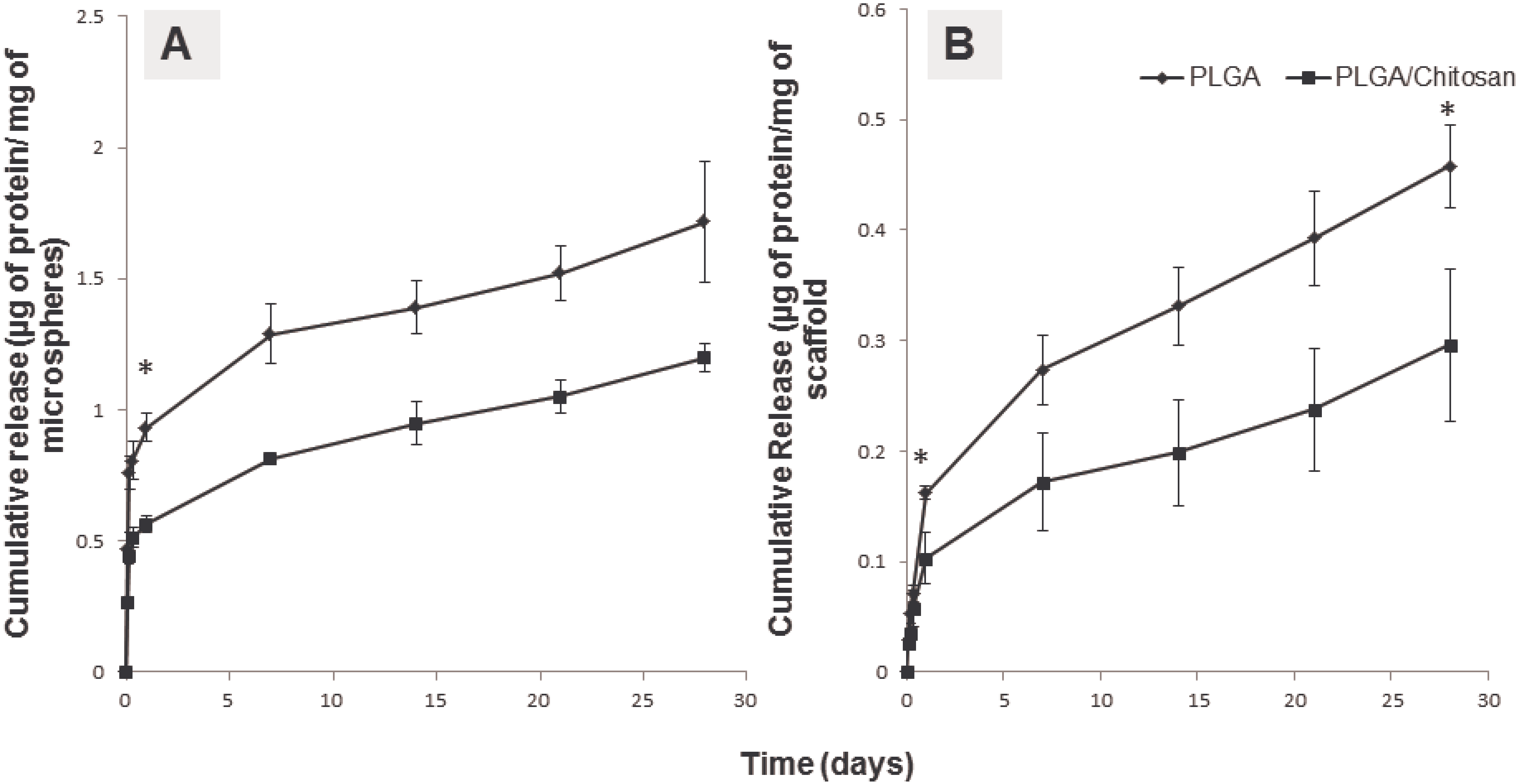
A
B
Cumulative release (µg of protein/ mg of microspheres)
Cumulative Release (µg of protein/mg of scaffold
PLGA
PLGA/Chitosan
*
0
0.5
1
1.5
2
2.5
0.1
0.2
0.3
0.4
0.5
0.6
5
10
15
20
25
30
Time (days)

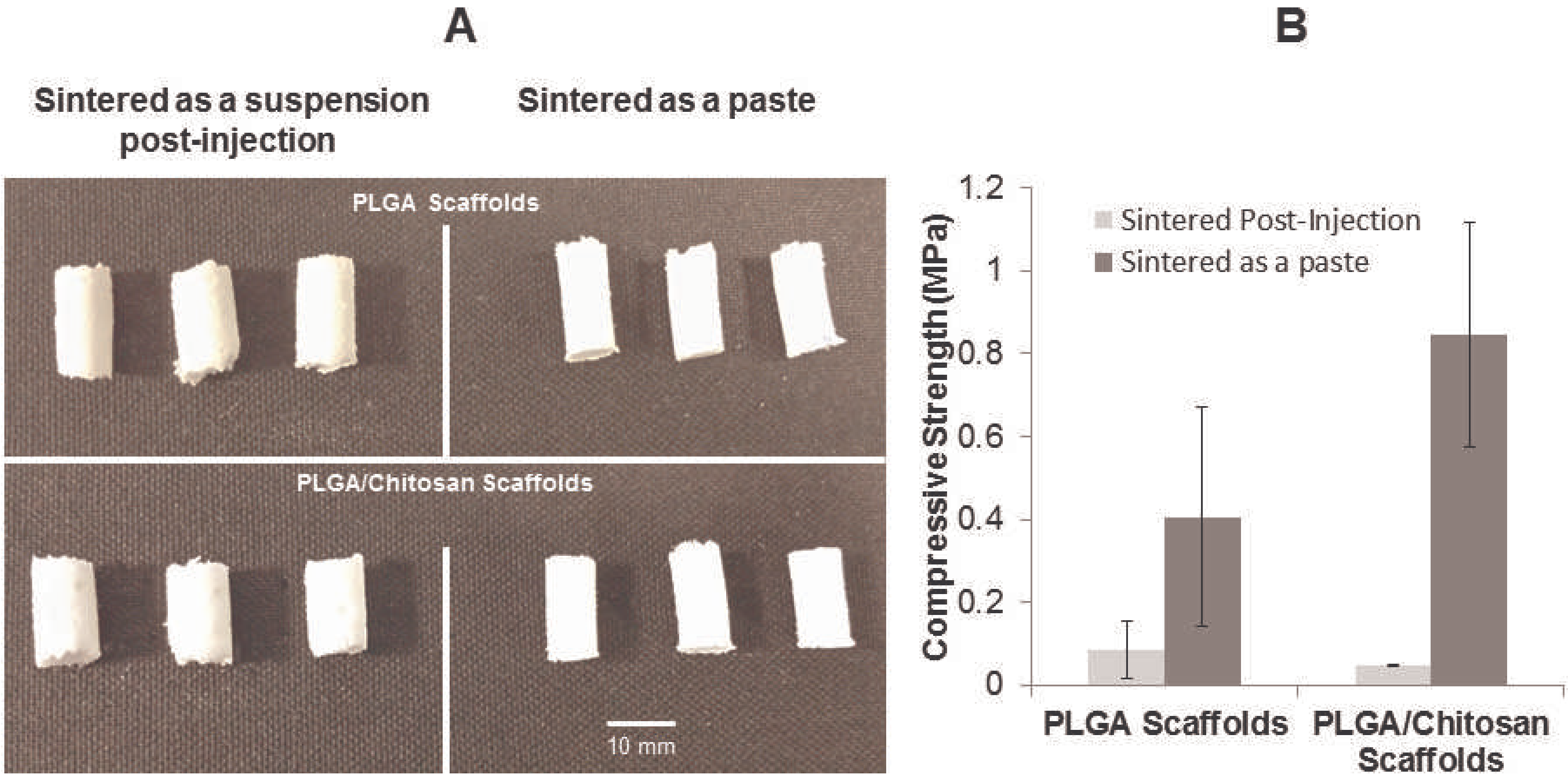
A
B
Sintered as a suspension post-injection
Sintered as a paste
PLGA Scaffolds
PLGA/Chitosan Scaffolds
10 mm
Compressive Strength (MPa)
1.2
1
0.8
0.6
0.4
0.2
0
Sintered Post-Injection
Sintered as a paste
PLGA Scaffolds
PLGA/Chitosan Scaffolds

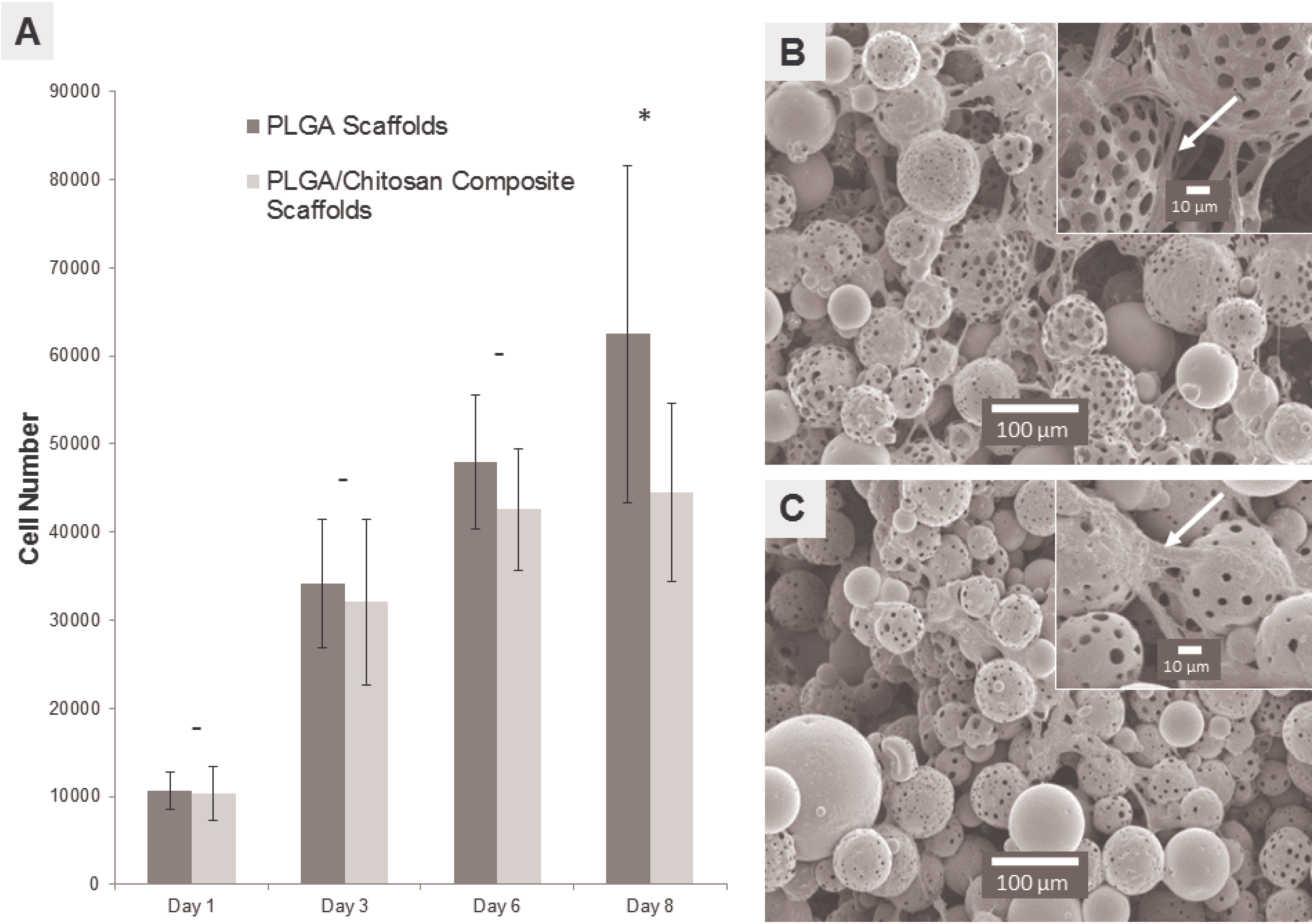
A
B
C
PLGA Scaffolds
PLGA/Chitosan Composite Scaffolds
Cell Number
90000
80000
70000
60000
50000
40000
30000
20000
10000
0
Day 1
Day 3
Day 6
Day 8
*
100 µm
10 µm
100 µm
10 µm

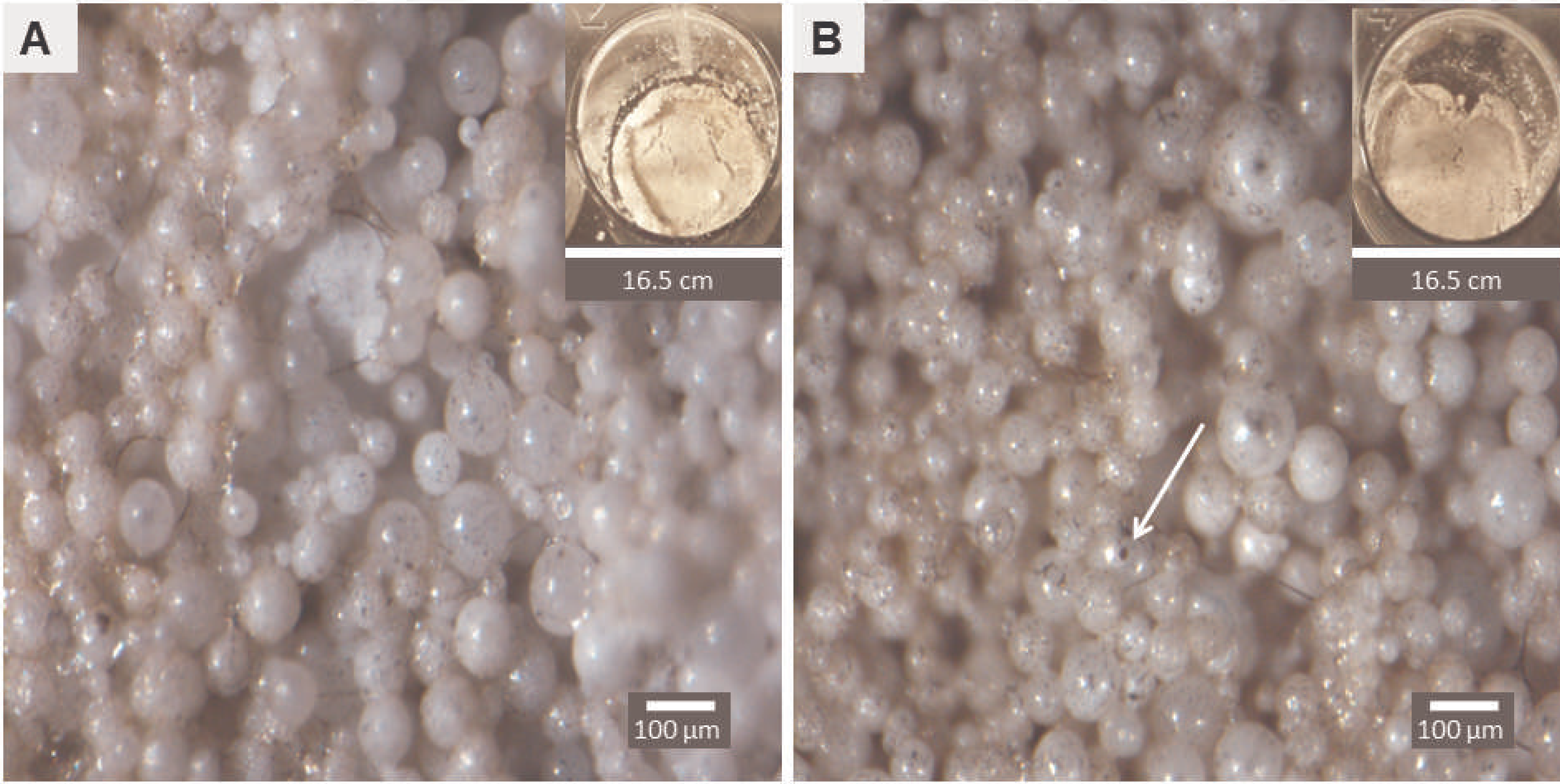
A
16.5 cm
100 µm
B
16.5 cm
100 µm

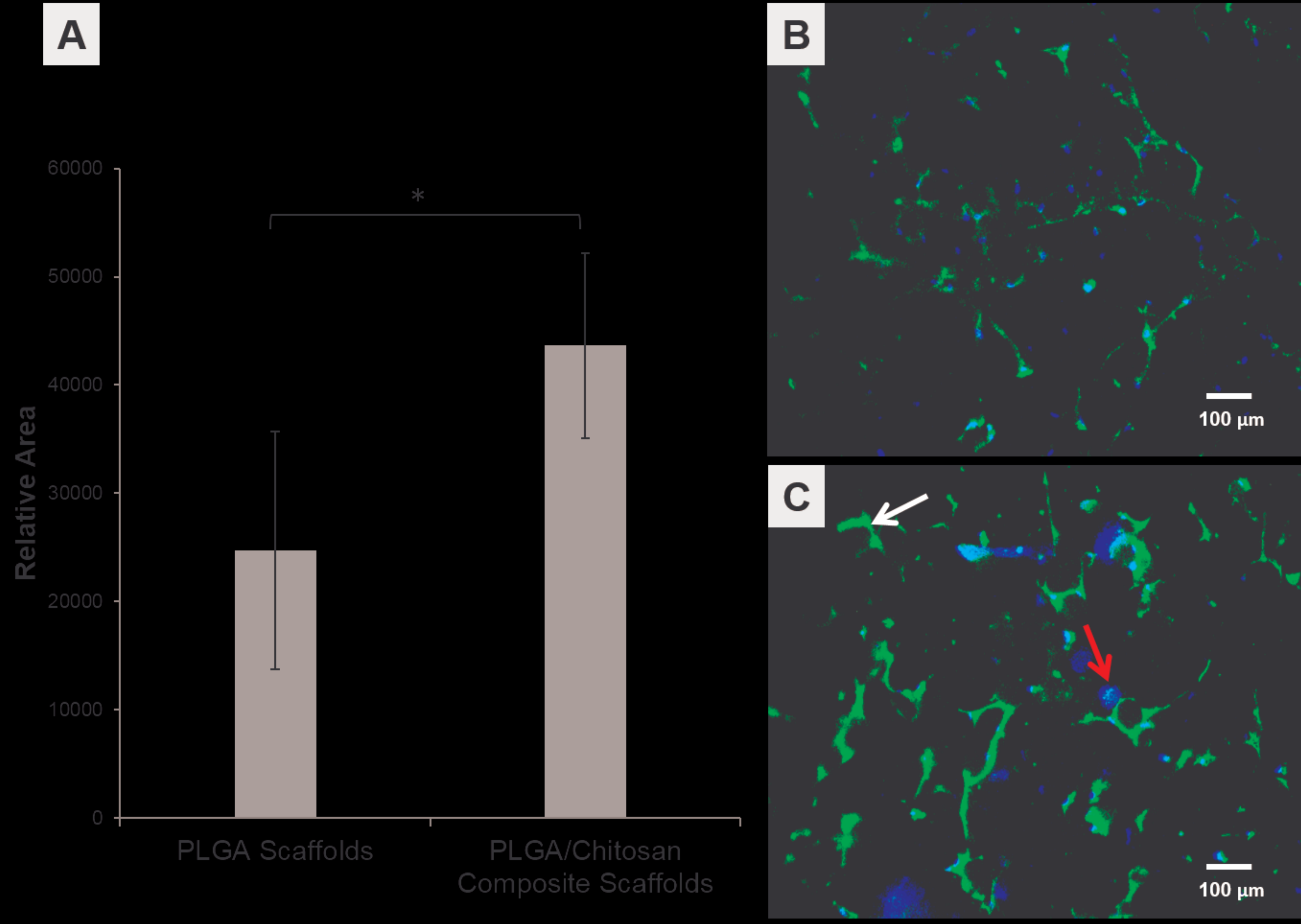

A
B
C
60000
50000
40000
30000
20000
10000
0
Relative Area
*
PLGA Scaffolds
PLGA/Chitosan Composite Scaffolds
100 μm
100 μm